Global bifurcations of a periodically forced biological oscillator

Leon Glass, Michael R. Guevara, Jacques Belair, and Alvin Shrier
Department of Physiology, McGill University, McIntyre Medical Sciences Building, 3655 Drummond Street, Montreal, Quebec H3G 1Y6, Canada
(Received 12 September 1983)

A single brief current pulse delivered to a spontaneously beating aggregate of cardiac cells from embryonic chick heart will reset the rhythm of the aggregate. The resetting depends on both the magnitude of the stimulus and the phase in the cycle at which the stimulus is delivered. Experimental data on resetting are fitted to an analytic function. This function, in turn, is used to construct a first return or Poincaré map which can be iterated to predict the effects of periodic pulsatile stimulation for any particular combination of frequency and amplitude of the stimulation. As the stimulation strength is increased the Poincaré map changes from a monotonic circle map of degree 1 to a nonmonotonic circle map of degree 1. The bifurcations in the frequency-amplitude parameter space are determined numerically by iterating the Poincaré map, and are compared with bifurcations in a simple model map and with those experimentally observed. These systems display period-doubling, intermittent, and quasiperiodic dynamics. Universal features of the bifurcations in the frequency-amplitude parameter space are described.

I. INTRODUCTION

There is currently great interest in the transition from regular periodic dynamics to irregular "chaotic" dynamics in diverse physical and biological systems.[1] Two main concepts have evolved: (1) In many systems the dynamics can be well approximated by the one-dimensional deterministic finite-difference equation $x_i = f(x_{i-1})$, where f is a nonlinear function depending on one or more parameters; (2) the bifurcations (changes in the qualitative nature of the dynamics) which are observed under parametric changes seem to depend mainly on the topological properties of f. Here, we analyze the experimentally observed dynamics resulting from periodic stimulation of spontaneously beating aggregates of embryonic chick heart cells by reducing the problem to an analysis of the bifurcations of two-parameter one-dimensional finite-difference equations.

Most theoretical work to date on one-dimensional difference equations has considered the situation in which f is a one-parameter function with a single maximum which maps the unit interval into itself. There are certain features observed in the bifurcation structure of the dynamics under parametric changes which do not depend on the detailed functional form of f. For example, for $f(x)=\lambda x(1-x)$, as λ increases from 0 to 4, one observes that stable periodic orbits are encountered in a well-defined sequence, called the U sequence.[2] The U sequence contains successive period doublings which have been described by a renormalization group.[3] In physical situations involving chemical oscillators[4] and nonlinear electronic oscillators[5] which are modeled by interval maps, theoretical predictions based on the U sequence and the renormalization group have been experimentally confirmed.

In many instances, and, in particular, in situations involving periodic forcing of nonlinear oscillators, the dynamics can be described by a continuous nonlinear function f which maps the unit circle into itself. Such functions, sometimes called circle maps, have been proposed as models for periodically forced limit-cycle oscillators,[6,7] sinusoidally modulated Josephson junctions,[8] hybrid optical devices,[9] and periodically stimulated biological[10–15] and chemical[16] oscillators. A circle map can be classified by its (topological) degree. The degree of a circle map f counts the number of times f winds around the unit circle as the argument of f traverses the unit circle once. If f is of degree 1 and monotonic, then the bifurcations found under parametric changes are well understood.[17] A recent application of the renormalization group has treated the case in which f is of degree 1 at the transition point from monotonicity to nonmonotonicity.[18] Although the situation in which f is nonmonotonic has been considered in several recent papers,[6,19–24] much less is known about the bifurcations in this circumstance. In our experiments, nonmonotonic, degree-1 circle maps are found; therefore, understanding the bifurcations of these maps is crucial to understanding the observed dynamics.

This paper gives a detailed analysis of the bifurcations observed during periodic stimulation of chick heart cells as the strength and frequency of the periodic stimulation are varied. We compare the dynamics experimentally observed with the dynamics predicted by iterating experimentally derived, one-dimensional circle maps. The close agreement between the experiment and theory lends further support to the hypothesis that the dynamics of periodically stimulated cardiac cells can be described by circle maps. We also evaluate, from numerical studies, the possibility for universal bifurcations of two-parameter circle maps.

In Sec. II we describe the general theory and review previous results. In Sec. III we propose a functional form for the circle maps for periodically stimulated spontaneously active cardiac cells which enables us to carry out numeri-

cal studies of the bifurcations. The bifurcation structure is described in Sec. IV. The results are discussed in Sec. V.

II. THEORY

We assume that the spontaneous beating of chick heart cells can be represented by a strongly attracting limit-cycle oscillation. The response of this system to single and periodic perturbations has been discussed recently,[13] and, hence, will only briefly be reviewed.

Assume the limit cycle has period T_0 with initial conditions $y(t=0)=y_0$, with y_0 being an arbitrary point on the limit cycle. Then the phase ϕ $(0\leq\phi<1)$ of any point $y(t)$ on the cycle is defined to be t/T_0 (mod 1). Let $y(t=0)$ and $y'(t=0)$ be the initial conditions of a point on the cycle and a point not on the cycle, respectively; and let $y(t)$ and $y'(t)$ be the coordinates of the trajectories at time t. If

$$\lim_{t\to\infty} d(y(t),y'(t))=0 ,$$

where d is the Euclidean distance, then the eventual phase of $y'(t=0)$ is defined to be the phase of $y(t=0)$. A locus of points all with the same eventual phase is called an isochron.

A brief stimulus delivered at a phase ϕ perturbs the oscillation from the isochron at phase ϕ to the isochron with new phase ϕ',

$$\phi'=g(\phi) , \tag{1}$$

where $g(\phi)$ is called the phase transition curve (PTC). Define the cycle length to be the time between two successive marker events of an oscillation. If the length of a perturbed cycle is T, and if the return to the limit cycle following a perturbation is sufficiently rapid,

$$T/T_0=1+\phi-g(\phi) . \tag{2}$$

Consequently, the PTC can be determined once T/T_0 is experimentally measured as a function of ϕ.

Now assume that during periodic stimulation by brief-duration stimuli the properties of the oscillator are not changed, and that the return to the cycle is rapid compared to the time between consecutive stimuli. Calling ϕ_i $(0\leq\phi_i<1)$ the phase of the oscillator just before delivery of the ith stimulus and t_s the time between successive stimuli,[25] we then have

$$\phi_{i+1}=f(\phi_i)=g(\phi_i)+\tau \pmod 1 \tag{3}$$

where $\tau=t_s/T_0$ is the normalized period between stimuli. Iteration of Eq. (3) (called the first return or Poincaré map) generates the sequence ϕ_0, $\phi_1=f(\phi_0)$, $\phi_2=f(\phi_1)=f^2(\phi_0),\ldots,\phi_N=f^N(\phi_0)$. The cycle of period N consists of N points $\phi_1^*,\phi_2^*,\ldots,\phi_N^*$ satisfying $\phi_{i+N}^*=\phi_i^*$, $\phi_{i+j}^*\neq\phi_i^*$ for $j=1,2,\ldots,N-1$, and is stable, provided that $\left|\partial f^N/\partial\phi_i\right|_{\phi_i^*}<1$. If an extremum of f is on a cycle, the cycle is called superstable. The locus of superstable cycles in parameter space is called the skeleton. Stable cycles of Eq. (3) correspond to stable phase-locked solutions of the forced oscillator. A period-N cycle of Eq. (3) corresponds to $N:M$ phase locking where

$$M=\sum_{i=1}^{N}\Delta\phi_i^*,\quad \Delta\phi_i^*=g(\phi_i^*)-\phi_i^*+\tau . \tag{4}$$

The rotation number ρ is defined as

$$\rho=\lim_{j\to\infty}\sup\left[\frac{1}{j}\sum_{i=1}^{j}\Delta\phi_i\right] . \tag{5}$$

$N:M$ phase locking thus has $\rho=M/N$.

In general, the PTC, Eq. (1), will depend on the strength of the imposed stimulus. In our experiments, as stimulus strength increases the PTC changes from a monotonic degree-1 map to a nonmonotonic degree-1 map. When $f(\phi)$ is monotonic the rotation number is independent of the initial point, leading to phase-locked (ρ rational) or quasiperiodic (ρ irrational) dynamics.[17] In the strength-frequency parameter plane, values leading to a rational $\rho=q/p$ form a compact region called an Arnol'd tongue. When f is not monotonic, less complete results are available.[6,19–24] The rotation number may cover an interval, and stable periodic points of different periods can coexist.[6,19–24]

The "canonical" example of degree-1 circle maps is the sine map, defined as

$$\phi_{i+1}=f(\phi_i)=\phi_i+b\sin(2\pi\phi_i)+\tau . \tag{6}$$

Its bifurcation structure is schematically depicted in Figs. 1 and 2 which are based on results in Refs. 19–23. Each Arnol'd tongue, associated with $p:q$ phase locking splits into two branches as b is increased. Period-doubling bifurcations occur leading to $2p:2q$ phase locking. Higher-order bifurcations also occur leading to a complex geometrical structure. One way to represent the bifurcations is the skeleton. In Fig. 2 we show the skeleton associated with the rotation number $\rho=1$, up to cycles of period 4. A topologically equivalent skeleton was conjectured to arise in the Y-shaped region of each Arnol'd tongue.[19] This structure is also found in other two-parameter maps.[26,27] We propose that the topological structure in

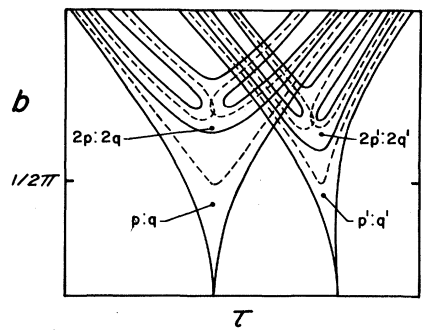

FIG. 1. Schematic representation of two Arnol'd tongues from Eq. (6) with rotation numbers q/p and q'/p'. The superstable cycles are shown by dashed lines. For $b<1/2\pi$ the sine map is monotonic and the structure described by Arnol'd of nonoverlapping tongues is found. For $b>1/2\pi$ there are superstable cycles, period-doubling bifurcations, and overlapping of Arnol'd tongues.

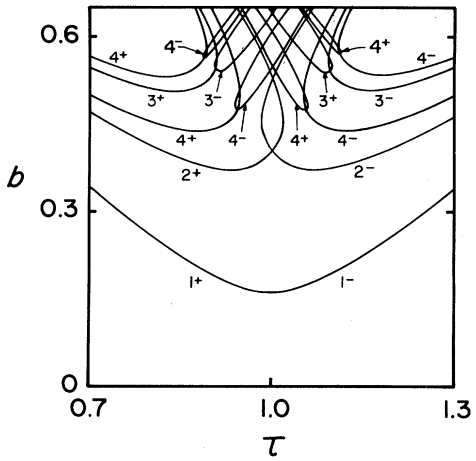

FIG. 2. Superstable cycles for Eq. (6) up to period 4 with $\rho=1$. Cycles derived from the maximum of the map are labeled by + whereas those derived from the minimum are labeled by − (redrawn from Ref. 19).

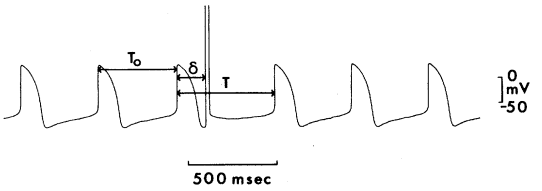

FIG. 3. One trial in a typical phase resetting experiment. A fine-tipped hollow glass microelectrode filled with electrolytic solution (3*M* KCl) is inserted into one cell of an aggregate 114 μm in diameter composed of approximately 800 spontaneously beating cells derived from embryonic chick heart. The electrode is used to record transmembrane voltage (which ranges from −80 to + 30 mV) and also to inject current pulses. An 8.8-nA current pulse of 20-msec duration delivered at a time δ after the third action potential upstroke gives rise to a prolonged cycle of length T. This pulse of current, since it flows through the large resistance (~30—80 MΩ) of the microelectrode, produces an off-scale rapidly rising and falling artifact in the voltage tracing. The phase of the stimulus is $\phi=\delta/T_0$, where T_0 is the duration of the immediately preceding unperturbed cycle. Aggregate No. 1.

Fig. 2 represents a "universal" feature of the bifurcations of two-parameter one-dimensional maps with two extrema and is thus a two-dimensional analog of the U sequence. For all circle maps of degree 1, we know that all Arnol'd tongues must extend into the region of parameter space in which the map becomes nonmonotonic.[19,23] However, we do not know if the two-dimensional bifurcation topology of Figs. 1 and 2 is found for other circle maps of degree 1.

III. PHASE TRANSITION CURVE (PTC)

Under the assumption that the cardiac oscillator is a strongly attracting limit-cycle oscillator with rapid relaxation back to the cycle following a perturbation, it is only necessary to know the PTC, Eq. (1), in order to compute the effects of periodic stimulation. Some work has been done using model functions for the PTC, such as the sine function[11,19] or piecewise-linear functions.[11,28,29] Alternatively, mathematical models are assumed for the limit-cycle oscillation and the PTC's are either analytically[12,30] or numerically[14,31] computed.

In our original study, a region of the experimentally obtained PTC which shows a maximum and a minimum was fit to a quartic polynomial, and numerical studies of the phase-locking regions were carried out.[10] To extend this earlier work it is necessary to obtain an analytic expression for the entire PTC as a function of parameter strength.

An experiment used to determine the PTC is shown in Fig. 3. The potential difference across the membrane of one cell in an aggregate of electrically coupled spontaneously beating embryonic cardiac cells is recorded with a microelectrode. The preparation and properties of the aggregates have been detailed previously.[32] The upstroke of the action potential is assigned a phase of zero. At a phase $\phi=\delta/T_0$, where δ is the time after the upstroke and T_0 is the intrinsic cycle length, following every tenth action potential, a brief pulse of current is delivered through the microelectrode leading to a perturbed cycle length T. For perturbations delivered sufficiently late in the cycle, the stimulus leads to an action potential upstroke sometime during the stimulus artifact itself so that T cannot be precisely measured.

Figure 4 shows plots of the normalized perturbed cycle length T/T_0 arranged in order of increasing perturbation strength [strength increases from Figs. 4(a) to 4(e)]. The most complete set of data from one aggregate is shown by the closed circles in Figs. 4(c), 4(d), and 4(e). These three levels of stimulation were obtained by setting the amplitude control of the stimulator to 0.06, 0.08, and 0.10, respectively (arbitrary units). The stimulus amplitude parameter A is taken to be 0.06, 0.08, and 0.10 in Figs. 4(c), 4(d), and 4(e), respectively. Data in Figs. 4(a) and 4(b) were selected to demonstrate a progression in the shape of the T/T_0 curve from Figs. 4(a) to 4(e) that is typical of that seen in many experiments. We assign values of the stimulus amplitude parameter A of 0.02 and 0.04 to Figs. 4(a) and 4(b), respectively, so that the value of A in Figs. 4(a) through 4(e) falls in the ratios 1:2:3:4:5. Over the most interesting region, from the standpoint of this work [Figs. 4(c), 4(d), and 4(e)], this assumption is well supported by the experimentally measured current amplitudes within a given aggregate [5.2, 6.8, and 8.8 nA for the closed circles of 4(c), 4(d), and 4(e), respectively; 8.7 and 11.0 nA for the open circles of 4(d) and 4(e), respectively]. Since the number of cells (and hence the amount of current needed to charge the capacitance of the total membrane area) and the electrophysiological properties vary from aggregate to aggregate, the current pulse amplitude is not the same for both sets of data in each panel of Fig. 4.

We assume that the normalized perturbed cycle length T/T_0 is given by

$$T/T_0=1+U_1(\phi)+U_2(\phi)\,, \tag{7a}$$

where

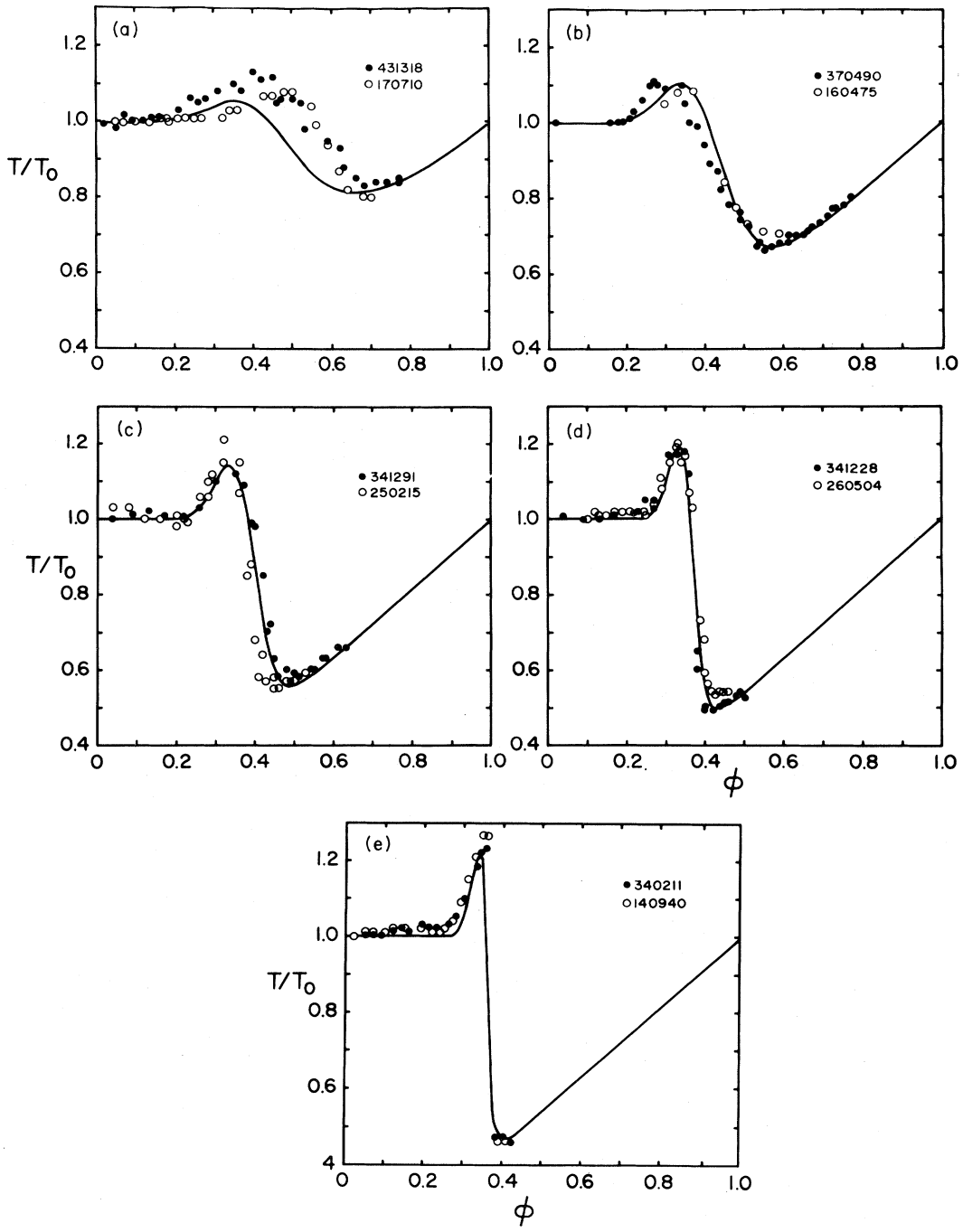

FIG. 4. Experimentally measured curves showing perturbed cycle length T/T_0 as a function of phase $\phi=\delta/T_0$ of delivery of the stimulus. The effective pulse amplitude increases in (a) through (e) (see text). The code numbers are our internal codes. Solid lines represent functions fitted using Eq. (7). Since the stimulus artifact obscures the action potential upstroke for stimuli delivered late in the cycle, T/T_0 data points for late cycle phases cannot be exactly given. However, the experimental points are closely approximated by the fitted curve. Pairs of sets of data points in (a)—(e), respectively, are from different aggregates and were selected on the basis of their similar appearance. Aggregate No. 1 (diameter is 114 μm): (c), (d), and (e) (closed symbols); pulse amplitude 5.2, 6.8, 8.8 nA; pulse duration 20 msec. Aggregate No. 2 (diameter is 181 μm): (c) and (d) (open symbols); pulse amplitude 8.7, 11.0 nA; pulse duration 20 msec. Aggregate No. 3 (diameter is 171 μm): panel (a) (open symbols); pulse amplitude 4.6 nA; pulse duration 20 msec. Aggregate No. 4 (diameter is 171 μm): panel (a) (closed symbols); pulse amplitude 3.2 nA; pulse duration 20 msec. Aggregate No. 5 (diameter is 228 μm): panel (b) (open symbols); pulse amplitude 14.1 nA; pulse duration 10 msec. Aggregate No. 6 (diameter is 105 μm): panel (b) (closed symbols); pulse amplitude 3.1 nA; pulse duration 20 msec. Aggregate No. 7 (diameter is 190 μm): panel (e) (open symbols); pulse amplitude, 23.8 nA; pulse duration 20 msec. In aggregates Nos. 3, 5, and 7 the current was injected in a switched mode at a frequency of 1 kHz. The currents quoted for these aggregates are the effective currents.

TABLE I. Qualitative dependence of T/T_0 vs ϕ curve on individual parameters.

Characteristic of T/T_0 curve (Fig. 4)	Parameter most directly related	Change in parameter as stimulus strength increases
height of maximum	C	↑
position of maximum	ϕ_{max}	↓
width of maximum	σ^2	↓
crossover from prolongation to shortening of cycle length	θ	↓
magnitude of slope at crossover	n	↑
slope of T/T_0 for $\theta<\phi<1$	S	

$$U_1(\phi)=C\exp\left[-\frac{(\phi-\phi_{max})^2}{\sigma^2}\right],\quad U_2(\phi)=\frac{S(\phi-1)\phi^n}{\theta^n+\phi^n} \tag{7b}$$

and C, ϕ_{max}, σ, S, θ, and n are parameters which depend on stimulus strength. These functions were chosen to empirically "fit" the data. The dependence of the shape of the T/T_0 curves on the individual parameters is summarized in Table I.

The function U_1 largely gives the region of the curves in Fig. 4 in which T/T_0 exceeds 1. As the stimulus strength increases, Fig. 4 shows that the position of the maximum (approximately at ϕ_{max}) moves to lower values of ϕ, the height of the maximum (approximately $1+C$) increases slowly, and the half-width of the peak [approximately $2(\ln 2)^{1/2}\sigma$] decreases. Therefore, the parameters in U_1 can be estimated by considering the position, height and half-width of the maximum in Fig. 4. (Since the term U_2 also influences these values, only approximations for C, ϕ_{max}, and σ can be made in this fashion.)

In the asymptotic limit $n\to\infty$, U_2 is a piecewise-linear function with $U_2=0$ for $0\le\phi<\theta$ and $U_2=S(\phi-1)$ for $\theta<\phi<1$. Figure 4 shows that increasing stimulus strength leads to an earlier crossover from interbeat prolongation to interbeat shortening (decreasing θ), but a steeper slope at this transition point and a deeper minimum (increasing n). However, the slope of the T/T_0 vs ϕ curve for ϕ sufficiently large does not change appreciably for increasing stimulus strength (constant S) and is discontinuous at $\phi=0$.

The quantitative determination of the parameters in Eq. (7) was carried out in two steps. First an attempt was made to separately fit each of the five sets of data given by the closed circles in Fig. 4 to Eq. (7). Parameters could be readily estimated using the considerations outlined above. The parameters determined in this fashion are shown in Table II in parentheses. Next, an attempt was made to see if the parameters could be continuously fit to simple functions of the stimulus strength A. All the parameters shared an approximate linear or exponential dependence on A. Setting $\bar{A}=A/0.02$, we obtain

$$\begin{aligned} &C=0.125+0.025\bar{A},\quad \phi_{max}=0.34+0.12\times 2^{-\bar{A}},\\ &\sigma^2=0.04\times 2^{-\bar{A}},\quad \theta=0.34+0.48\times 2^{-\bar{A}},\\ &n=1.875\times 2^{\bar{A}},\quad S=0.92. \end{aligned} \tag{8}$$

There is a marked discrepancy between the data and the theoretical fit using Eqs. (7) and (8) at the lowest stimulus strength considered [Fig. 4(a), $A=0.02$]. At lower current strengths [i.e., 4(a) and 4(b)], the topological properties of the phase locking are not sensitive to quantitative details of the T/T_0 curve since the PTC is monotonic. Therefore, approximations to the PTC at lower current strengths do not affect the conclusions of this work. In fitting the data we have given much more emphasis to the points with $A\ge 0.06$ [Figs. 4(c)—4(e)]. In this range there are complex bifurcations and our experimental data are more complete than for $A<0.06$.

At the highest stimulus strength it appears the data are discontinuous in the neighborhood of the value $\phi=\theta$ [Fig. 4(e)]. This type of behavior occurs in models in which the PTC undergoes an abrupt transition from degree 1 to degree 0.[12,30] However, it is very difficult to establish experimentally whether the data are continuous or discontinuous. Because of the possibility that the response does become discontinuous, extrapolation of the functions in Eq. (7) to higher stimulus will not be pursued further in this report.

Despite these reservations, there is excellent agreement between the numerically fit curves in Fig. 4 and the experimental data. At the moment, we cannot derive the func-

TABLE II. Values of parameters in Eq. (9) for the curves shown in Fig. 4. Values in parentheses were estimated as described in the text. Values not in parentheses are the values from Eq. (8).

Parameter	Stimulus strength (A)				
	0.02	0.04	0.06	0.08	0.10
C	0.15	0.175	0.20	0.225	0.25
	(0.15)	(0.15)	(0.15)	(0.20)	(0.20)
ϕ_{max}	0.40	0.37	0.355	0.3475	0.34375
	(0.40)	(0.36)	(0.36)	(0.34)	(0.34)
σ^2	0.02	0.01	0.005	0.0025	0.00125
	(0.025)	(0.0075)	(0.005)	(0.0025)	(0.001)
θ	0.58	0.46	0.40	0.37	0.355
	(0.65)	(0.44)	(0.42)	(0.37)	(0.36)
n	3.75	7.5	15.0	30.0	60.0
	(5.00)	(7.0)	(15.0)	(30.0)	(50.0)
S	0.92	0.92	0.92	0.92	0.92
	(0.92)	(0.92)	(0.92)	(0.92)	(0.92)

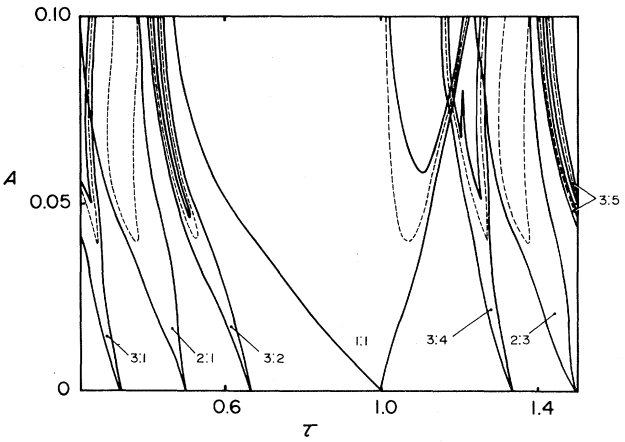

FIG. 5. Principal phase-locking regions (enclosed by solid lines) and associated superstable cycles (dashed lines) numerically computed from Eq. (9). For values of A between 0 and 0.02, ϕ_{max}, σ^2, θ, and n were held at their value for $A=0.02$ and C and S were linearly interpolated between 0 and the values of these parameters at $A=0.02$. From Eq. (9) one can show that if there is an N:M pattern for a given $\tau=\tau_0$ then for $\tau=\tau_0+j$ there will be a N:$M+Nj$ pattern (see Ref. 12).

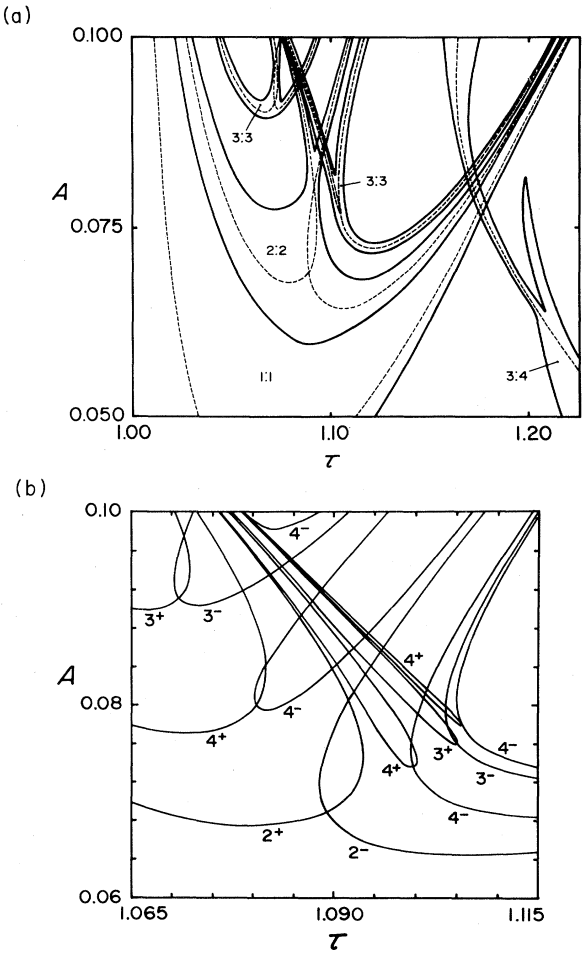

FIG. 6. Enlargement of a portion of Fig. 5 to show period-doubling and higher-order bifurcations with rotation number $\rho=1$. (a) 1:1, 2:2, and 3:3 phase-locking zones and associated period-1, -2, and -3 superstable cycles. (b) Superstable cycles with rotation number $\rho=1$.

tions used in Eqs. (7) and (8) from ionic models of cardiac activity; we consider these functions as convenient approximations which facilitate detailed iteration of the Poincaré map of Eq. (3).

IV. GLOBAL BIFURCATIONS

The main reason for deriving an analytic expression for the PTC was to enable us to compute in detail the theoretically predicted bifurcations of the periodically forced aggregate of cardiac cells. From Eqs. (2), (3), and (7a) we have

$$\phi_{i+1}=\phi_i-U_1(\phi_i)-U_2(\phi_i)+\tau \pmod 1 \qquad (9)$$

where U_1 and U_2 are given in Eqs. (7b) and (8) and τ is the time between successive stimuli normalized to the mean cycle length. Upon iteration, regions of stable phase locking, period-doubling bifurcations, bistability, and chaotic dynamics are found. The results are shown in Figs. 5 and 6. We first compare these results with the bifurcations found in the sine map of Eq. (6) (Figs. 1 and 2) and then with those observed in the experiments.

A. Comparison of the bifurcations of the fitted map with those of the sine map

For $0<A\lesssim 0.039$ the fitted PTC is monotonic. Consequently, in this region there is an Arnol'd tongue extending to $A=0.0$ for each rational rotation number. For $A\gtrsim 0.039$ there are two extrema in the PTC. Therefore, as in the sine map, for each rational rotation number there must be two superstable cycles at different values of τ.[19] This behavior is illustrated in Fig. 5. In addition, in some of the Arnol'd tongues we find that there is the same complex sequence of period-doubling bifurcations as observed in the sine map. This is illustrated in Fig. 6 which shows the period doubling associated with $\rho=1$. Bifurcations having an identical skeleton have also been observed in the tongues associated with period-3 orbits (3:1, 3:2, 3:4) but not in the tongues associated with period-2 orbits (2:1, 2:3). Bistability, associated with the crossing of Arnol'd tongues in the parameter plane is exemplified in Fig. 7 where both 3:4 and 2:2 phase locking are present ($A=0.08$, $\tau=1.172$). The bifurcations predicted for the periodically stimulated heart cells thus appear to be a subset of the bifurcations observed in the sine map. One possible reason that not all bifurcations are present is that the extrema of the PTC do not grow linearly with perturbation strength.

B. Comparison of the predictions of the fitted map with the experimental response to periodic stimulation

Periodic stimulation of spontaneously beating cardiac cells leads to a rich variety of different periodic and aperiodic dynamical activities (Figs. 8 and 9, respectively).

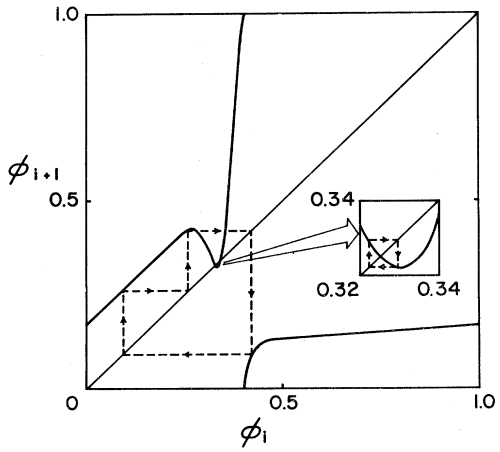

FIG. 7. A plot of ϕ_{i+1} vs ϕ_i from Eq. (9) with $A=0.08$ and $\tau=1.172$. There are two stable cycles corresponding to 3:4 and 2:2 phase locking (dashed lines). The inset shows an enlargement of the region near the local minimum.

The data indicating the different dynamics found at particular combinations of frequency and amplitude of stimulation are superimposed on the theoretically computed zones in Fig. 10. There are three values of stimulus strength. For $A=0.06$ and $A=0.10$ the entrainment data were collected from a single aggregate (aggregate No. 1) and the associated T/T_0 phase resetting data are shown in

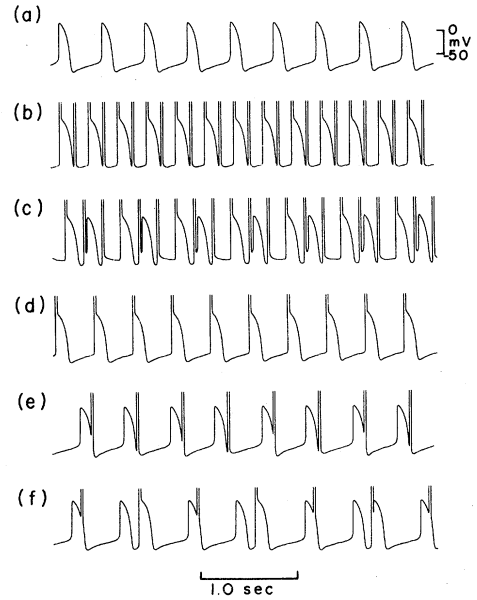

FIG. 8. Recordings of transmembrane potential showing regular dynamics (aggregate No. 1). The average interbeat interval t_{av} is computed from the five spontaneous interbeat intervals immediately preceding the start of each run, and $\tau=t_s/t_{av}$. (a) Control unperturbed activity. (b) $A=0.10$, $t_s=150$ msec, $t_{av}=469$ msec, $\tau=0.32$, 2:1 phase locking. (c) $A=0.10$, $t_s=190$ msec, $t_{av}=482$ msec, $\tau=0.39$, 3:2 phase locking. (d) $A=0.10$, $t_s=400$ msec, $t_{av}=437$ msec, $\tau=0.99$, 1:1 phase locking. (e) $A=0.10$, $t_s=470$ msec, $t_{av}=448$ msec, $\tau=1.05$, 2:2 phase locking. (f) $A=0.10$, $t_s=600$ msec, $t_{av}=471$ msec, $\tau=1.27$, 2:3 phase locking.

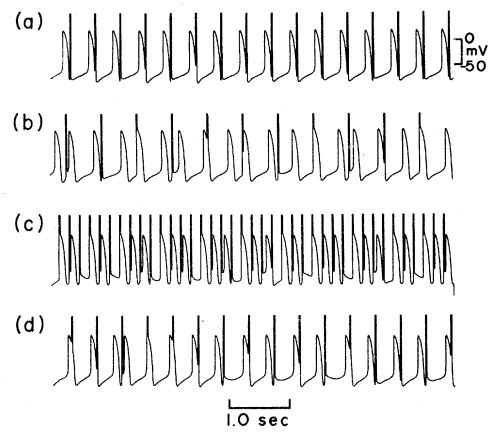

FIG. 9. Recordings of transmembrane potential which show fluctuating, irregular dynamics (aggregate No. 1). (a) $A=0.06$, $t_s=500$ msec, $t_{av}=475$ msec, $\tau=1.05$: dynamics resemble a 1:1 pattern with added noise. (b) $A=0.06$, $t_s=700$ msec, $t_{av}=484$ msec, $\tau=1.44$: dynamics are irregular, with apparently randomly inserted extra or escape beats that are not associated with a stimulus. (c) $A=0.10$, $t_s=200$ msec, $t_{av}=465$ msec, $\tau=0.43$: The dynamics are irregular with occasional dropped or skipped beats and resemble Wenckebach cardiac dysrhythmias. (d) $A=0.10$, $t_s=500$ msec, $t_{av}=437$ msec, $\tau=1.15$: dynamics are irregular, with occasional escape beats that are not associated with a stimulus.

Fig. 4 (runs 341 291 and 340 211, respectively). The data for $A=0.08$ were taken from a different preparation (aggregate No. 2). The associated T/T_0 data are also shown in Fig. 4 (run 260 504). The phase-locking patterns covering the largest areas in the (A,τ) parameter space (the 1:1, 2:1, and 2:3 patterns) are very easy to observe and maintain (Fig. 8). Other periodic patterns that cover smaller areas of the (A,τ) parameter space are more difficult to

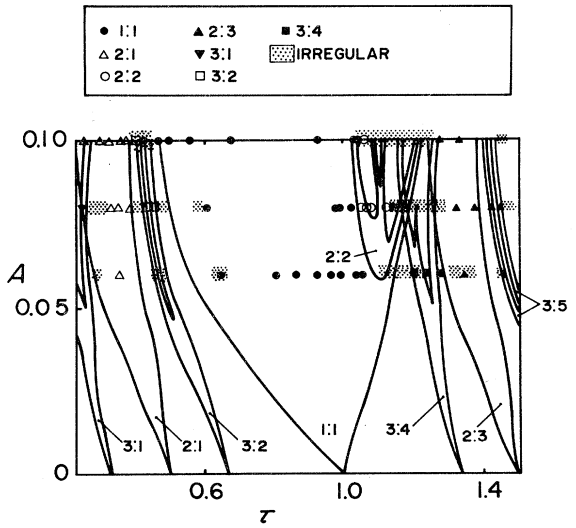

FIG. 10. A plot showing experimentally observed dynamics superimposed on theoretically computed phase-locking zones. Data from aggregate No. 1 are used for $A=0.06$ and $A=0.10$ and data from aggregate No. 2 are used for $A=0.08$.

observe. For example, in the region $1.05<\tau<1.4$, $0.06<A<1.0$, it is very difficult to obtain a stable phase-locked pattern.

In general, there is close correspondence between the dynamics observed experimentally and the boundaries theoretically computed using the data shown in Fig. 4. However, there are some discrepancies. Most striking is our inability to experimentally observe stable phase-locking zones which occupy small areas in the (A,τ) parameter space. The failure to observe the fine structure of phase locking theoretically predicted probably stems from small amounts of "noise" inherent in this biological preparation.[33]

One systematic discrepancy is in the location of the high-frequency (left-hand) boundary of the 1:1 phase-locking region. During periodic stimulation at a fixed frequency and amplitude near this boundary one typically has dynamics passing through a sequence of different patterns. Thus, as the stimulation progresses, one may observe the transitions 1:1→7:6→6:5→5:4→4:3 with all stimulation parameters held fixed. There is not an abrupt transition from one pattern to another and intermediate patterns and irregularity are often observed. This behavior is most likely due to a biological phenomenon called "overdrive suppression."[15] Following cessation of 1:1 phase locking at frequencies higher than the intrinsic frequency of the aggregate one observes a transient increase in the intrinsic period, which gradually returns back to control. Thus, as the stimulus is continually applied the intrinsic cycle length increases (corresponding to a decrease in τ in Fig. 10) and this leads to bifurcations in the dynamics.

Analyzing the dynamics over extended times during periodic stimulation provides further confirmation for the applicability of Eqs. (3) and (9) to the experiments. The basic idea is to determine directly from the data during periodic stimulation the plot of ϕ_{i+1} as a function of ϕ_i. This is done by measuring the time from the action potential immediately preceding a stimulus to that stimulus. That time is divided by the intrinsic cycle length, which is taken to be the average of the five spontaneous interbeat intervals immediately prior to the start of stimulation, to determine the phase of the stimulus.

In the first column of Fig. 11, ϕ_{i+1} is plotted as a function of ϕ_i for four runs, partial tracings of which are shown in Fig. 9. In the second column in Fig. 1, the function in Eq. (9) for the appropriate A and τ is superimposed on the experimental points.[34] Finally, in the last column of Fig. 11 are shown simulated dynamics assuming Eq. (9) with an added stochastic term generating uniformly distributed noise in an interval ± 0.015.

In Fig. 11, the superposition of Eq. (9) with the experimental points in the second column, and the close similarity of the simulated dynamics with the observed dynamics (compare columns 1 and 3) gives striking confirmation of the theory. The small discrepancies which are observed presumably reflect either inaccuracies in fitting the PTC to experimental data [for example, in the neighborhood of $\phi=0.38$ in Figs. 4(e) and 11(d)] or breakdown of the assumptions that allow representation of the dynamics by a one-dimensional difference equation.

Figure 11 also depicts three of the main postulated "routes to chaos."[1] In Figs. 11(a2) and 11(d2) there is a period-1 fixed point in the negative slope region of the Poincaré map. In Fig. 11(a2) this point is stable whereas in Fig. 11(d2) the point is unstable and one sees irregular dynamics such as are found in the "period-doubling" route to chaos.[1,3,10] Figure 11(c2) shows that the system is near a tangent bifurcaton on the period-1 map. This leads to "intermittency."[35] Finally, the dynamics in Fig. 11(b) clearly show density over the entire range of ϕ_i. In this case the map is not monotonic, and one has irregular dynamics similar to those expected on the "quasiperiodic" route to chaos.[18,20]

V. DISCUSSION

The present paper offers a concrete application of theoretical work on the bifurcations of circle maps to the field of cardiac electrophysiology. The theory was based on the assumption that the cardiac oscillation is a strongly attracting limit cycle which is being perturbed by electrical current pulses. Thus, the theory is equally applicable to other experimental systems in which an autonomous limit-cycle oscillation is perturbed by brief pulsatile stimuli. Periodic pulsatile stimulation of chemical and electronic oscillators which are strongly attracting limit cycles should lead to similar phenomena.

One of the motivations for this work was to determine if two-parameter circle maps would display universal bifurcations. Although robust results have appeared for monotonic circle maps[17] and for circle maps at the transition from monotonicity to nonmonotonicity,[18] the theory for nonmonotonic maps is still not well developed. Most work[19–23] to date has been for maps of the form

$$\phi_{i+1}=\phi_i+\tau+bp(\phi_i) \pmod 1 \tag{10}$$

where b and τ are constants and p is a function with $p(0)=p(1)$, with a single maximum and minimum in the interval [0, 1). The map used to predict the experimental response to periodic stimulation [Eq. (9)] does not follow this form. Therefore, theoretical studies of degree-1 circle maps more general than Eq. (10) are needed. However, the numerical studies do show that many of the main features of the sine map (Figs. 1 and 2) are also found in the predicted dynamics of the cardiac oscillator (Figs. 5 and 6). As well, overlapping of Arnol'd tongues is found in other two-parameter systems[36,37] and the complex period-doubling structures in Figs. 2 and 6 occur in other two-parameter maps with two extrema.[26,27] Thus, there is mounting evidence for universality in the bifurcations of maps of two parameters, but a complete theory is currently lacking.

In order to simplify this analysis we have not considered two important problems. (1) For many biological oscillators, there is a transition from a degree-1 PTC to a degree-0 PTC as stimulation strength is increased.[12,30] In the case of the heart cell aggregate, experimental and theoretical analysis of this transition is difficult and the subject of recent work.[38] The bifurcations found in the neighborhood of the transition from degree-1 to degree-0 circle maps are not well understood. (2) We assume

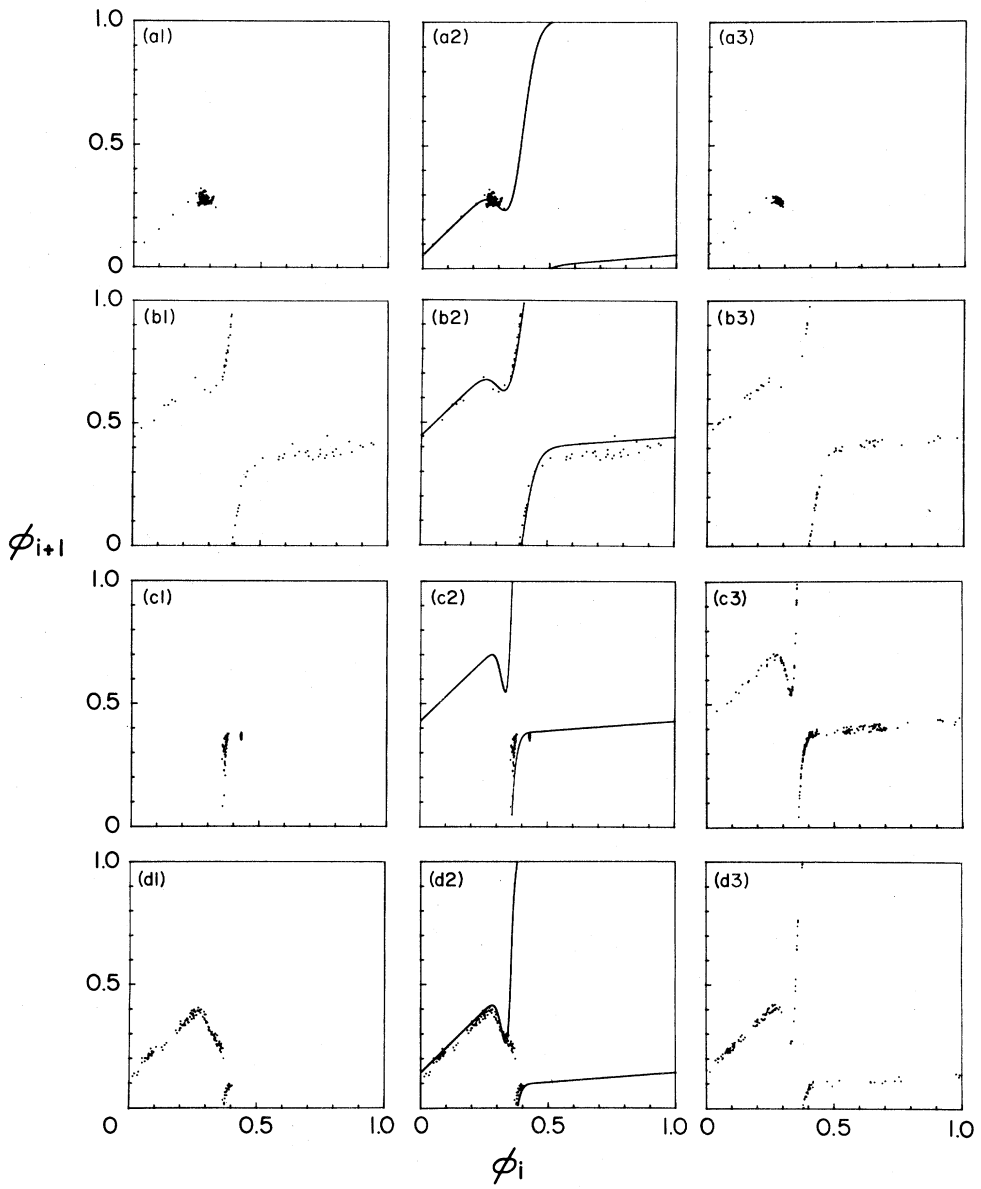

FIG. 11. Poincaré maps for four stimulation runs, portions of which are shown in Fig. 9, where row (a) here corresponds to row (a) in Fig. 9, and so forth. In the first column is shown ϕ_{i+1} vs ϕ_i determined from experimental data. In the second column, the Poincaré maps obtained from the single-pulse response [Eq. (9)] are superimposed on the experimental points. In the third column, the dynamics are simulated using Eq. (9) with noise added uniformly distributed in an interval of ± 0.015. The same initial condition and approximately the same number of stimuli are used in the simulated runs of the third column as in experimental data of the first column. In the experiment of row (c), two stimuli not separated by an action potential occasionally occurred [see Fig. 8(c)]. The phase of the second of such a pair of stimuli cannot be calculated. In (c1) only points for which ϕ_i and ϕ_{i+1} can be directly measured are included.

throughout that the relaxation back to the limit cycle is sufficiently rapid that a one-dimensional map is valid. Further analysis is needed to understand the connection between the bifurcation in this one-dimensional map and higher-dimensional maps which may be more accurate representations of the biological system.

Many pathological cardiac rhythms in man arise from the interactions of two or more autonomous pacemaker sites in the heart. As well, in patients with electronic pacemakers, brief electrical stimuli are periodically delivered directly to the cardiac tissue. Our experimental system provides a highly oversimplified model for these physiological situations. Since many of these complex systems are modeled by circle maps, we are led to conclude that the bifurcations and associated aperiodic dynamics observed in the iteration of circle maps may provide insight into the origin of the bizarre, erratic, and sometimes fatal cardiac dysrhythmias clinically observed.

ACKNOWLEDGEMENTS

This research has been supported by grants from the Natural Sciences and Engineering Research Council (NSERC) of Canada and the Canadian Heart Foundation. We thank Diane Colizza for expert technical assistance. M.R.G. is a recipient of a traineeship from the Canadian Heart Foundation. J.B. is a recipient of an NSERC fellowship.

[1]For reviews, see R. H. G. Helleman, in *Fundamental Problems in Statistical Mechanics,* edited by E. G. D. Cohen (North-Holland, Amsterdam, 1980), Vol. 5, p. 165; J. P. Eckmann, Rev. Mod. Phys. 53, 643 (1981); E. Ott, *ibid.* 53, 655 (1981); *Proceedings of the International Conference on Order in Chaos, Los Alamos, May, 1982,* edited by D. Campbell and H. Rose (North-Holland, Amsterdam, 1983).

[2]N. Metropolis, M. L. Stein, and P. R. Stein, J. Comb. Theory A 15, 25 (1973).

[3]M. J. Feigenbaum, J. Stat. Phys. 19, 25 (1978); 21, 669 (1979).

[4]A. S. Pikovsky, Phys. Lett. 85A, 13 (1981); R. H. Simoyi, A. Wolf, and H. L. Swinney, Phys. Rev. Lett. 49, 245 (1982).

[5]P. S. Linsay, Phys. Rev. Lett. 47, 1349 (1981); J. Testa, J. Pérez, and C. Jeffries, *ibid.* 48, 714 (1982); R. W. Rollins and E. R. Hunt, *ibid.* 49, 1295 (1982).

[6]J. Guckenheimer, in *Dynamical Systems, C.I.M.E. Lectures* (Birkhauser, Boston, 1980); M. Levi, Mem. Am. Math. Soc. 32, No. 244 (1981).

[7]G. M. Zaslavsky, Phys. Lett. 69A, 145 (1978); P. Coullet, C. Tresser, and A. Arneodo. *ibid.* 77A, 327 (1980); D. L. Gonzalez and O. Piro, Phys. Rev. Lett. 50, 870 (1983).

[8]T. Geisel and J. Nierwetburg, Phys. Rev. Lett. 48, 7 (1982); P. Bak, T. Bohr, M. H. Jensen, and P. V. Christiansen, Phys. Rev. B (to be published).

[9]K. Ikeda, Opt. Commun. 30, 257 (1979); K. Ikeda, H. Daido, and O. Akimoto, Phys. Rev. Lett. 45, 709 (1980); H. M. Gibbs, F. A. Hopf, D. L. Kaplan, and R. L. Shoemaker, *ibid.* 46, 474 (1981); P. Mandel and R. Kapral, Opt. Commun. 47, 151 (1983).

[10]M. R. Guevara, L. Glass, and A. Shrier, Science 214, 1350 (1981).

[11]N. Ikeda, H. Tsuruta, and T. Sato, Biol. Cybern. 42, 117 (1981).

[12]M. R. Guevara and L. Glass, J. Math. Biol. 14, 1 (1982); F. C. Hoppensteadt and J. Keener, *ibid.* 15, 339 (1982).

[13]L. Glass, M. R. Guevara, A. Shrier, and R. Perez, Physica (Utrecht) 7D, 89 (1983).

[14]M. Guevara, L. Glass, M. C. Mackey, and A. S. Shrier, I.E.E.E., Trans. Syst. Man Cybern. (to be published).

[15]D. L. Ypey, W. P. M. vanMeerwijk, and R. L. DeHaan, in *Cardiac Rate and Rhythm,* edited by L. N. Bouman and H. J. Jongsma (Martinus Nijhoff, The Hague, 1982), p. 363.

[16]E. Dulos and P. DeKepper, Biophys. Chem. (to be published).

[17]V. I. Arnol'd, Transl. Am. Math. Soc., 2nd Ser. 46, 213 (1965); M. R. Herman, *Geometry and Topology,* Lecture Notes in Mathematics No. 597 (Springer, Berlin, 1977), p. 271.

[18]M. J. Feigenbaum, L. P. Kadanoff, and S. J. Shenker, Physica (Utrecht) 5D, 370 (1982); D. Rand, S. Ostlund, J. Sethna, and E. D. Siggia, Phys. Rev. Lett. 49, 132 (1982); S. J. Shenker, Physica (Utrecht) 5D, 405 (1982).

[19]L. Glass and R. Perez, Phys. Rev. Lett. 48, 1772 (1982); R. Perez and L. Glass, Phys. Lett. 90A, 441 (1982).

[20]K. Kaneko, Prog. Theor. Phys. 68, 669 (1982); 69, 403 (1983).

[21]M. Schell, S. Fraser, and R. Kapral, Phys. Rev. A 28, 373 (1983).

[22]L. P. Kadanoff, J. Stat. Phys. 31, 1 (1983).

[23]P. Boyland, Ph.D. Thesis, University of Iowa, 1983 (unpublished).

[24]J. Palis, F. Takens, and S. Newhouse, Publ. Inst. Hauts Etud. Sci. 57, 5 (1983); C. Bernhardt, Proc. London Math. Soc. 3rd Ser. 45, part 2, 258 (1982); R. Ito, Math. Proc. Camb. Phil. Soc. 89, 107 (1981).

[25]D. H. Perkel, J. H. Schulman, T. H. Bullock, G. P. Moore, and J. P. Segundo, Science 145, 61 (1964).

[26]J. Belair and L. Glass, Phys. Lett. 96A, 113 (1983).

[27]S. Fraser and R. Kapral, Phys. Rev. A 25, 3223 (1982).

[28]G. K. Moe, J. Jalife, W. J. Mueller, and B. Moe, Circulation 56, 968 (1977).

[29]J. P. Segundo, Biol. Cybern. 35, 55 (1979).

[30]A. T. Winfree, Phys. Today 28, No. 3, 34 (1975); A. T. Winfree, *The Geometry of Biological Time* (Springer, New York, 1980).

[31]S. W. Scott, Ph.D. Thesis, SUNY at Buffalo (1979); E. N. Best, Biophys. J. 27, 87 (1979).

[32]J. R. Clay and A. Shrier, J. Physiol. 312, 471 (1981); D. Colizza, M. R. Guevara, and A. Shrier, Can. J. Physiol. Pharmacol. 61, 408 (1983).

[33]J. R. Clay, L. J. DeFelice, and R. L. DeHaan. Biophys. J. 28, 169 (1979); L. Glass, C. Graves, G. A. Petrillo, and M. C. Mackey, J. Theor. Biol. 86, 455 (1980); J. P. Crutchfield and B. A. Huberman, Phys. Lett. 77A, 407 (1980); R. Guttman, L. Feldman, and E. Jakobsson, J. Memb. Biol. 56, 9 (1980); G. Mayer-Kress and H. Haken, J. Stat. Phys. 26, 149 (1981); J. Perez and C. Jeffries, Phys. Rev. B 26, 3460 (1982).

[34]In the run displayed in Fig. 9(c) there are often two consecutive stimuli without an intervening action potential. Therefore, the phase ϕ_i of the second of the two consecutive stimuli is not measurable. In Fig. 11(c1) only the points for which both ϕ_i and ϕ_{i+1} are defined are plotted.

[35]P. Manneville and Y. Pomeau, Phys. Lett. 75A, 1 (1979); Commun. Math. Phys. 74, 189 (1980); Physica (Utrecht) 1D, 219 (1980); J. E. Hirsch, B. A. Huberman, and D. J. Scalapino, Phys. Rev. A 25, 519 (1982); C. Jeffries and J. Perez, *ibid.* 26, 2117 (1982).

[36]C. Hayashi, *Nonlinear Oscillations in Physical Systems* (McGraw-Hill, New York, 1964); J. Grasman, E. J. M. Veling, and G. M. Willems, SIAM J. Appl. Math. 31, 667 (1976); J. E. Flaherty and F. C. Hoppensteadt, Stud. Appl. Math. 58, 5 (1978).

[37]D. G. Aronson, M. A. Chory, G. R. Hall, and R. P. McGehee, Commun. Math. Phys. 83, 303 (1982).

[38]J. R. Clay, M. R. Guevara, and A. Shrier, Biophys. J. (to be published).